Bulletin of Volcanology (2019) 81: 71
https://doi.org/10.1007/s00445-019-1337-2

RESEARCH ARTICLE

El Escondido tuff cone (38 ka): a hidden history of monogenetic eruptions in the northernmost volcanic chain in the Colombian Andes

L. Sánchez-Torres[1,2] · A. Toro[3] · H. Murcia[1,4] · C. Borrero[5] · R. Delgado[3] · J. Gómez-Arango[6]

Received: 17 October 2019 / Accepted: 8 November 2019 / Published online: 26 November 2019

Abstract
El Escondido is a dacitic monogenetic volcano situated in the Samaná monogenetic volcanic field, within the Central Cordillera of Colombia. The tuff cone was emplaced in a deeply incised and rainy mountainous zone, ca. 38 ky ago by an explosive eruption that affected not only the metamorphic and igneous basement but also the remnants of the ~ 154 ka Pela Huevos volcano. The El Escondido volcaniclastic deposits are composed of juvenile pumice and lithic fragments including dense volcanic rocks from the Pela Huevos volcano, as well as metamorphic and igneous rocks from the basement. The pumice shows tubes and spongy textures. The volcanic lithics are dominantly angular and fresh, and exhibit different mineralogy and whole-rock geochemistry in comparison to the pumice. Plagioclase and amphibole are ubiquitous; however, biotite and quartz crystals occur only in the pumice fragments (~ 70 wt% SiO_2 volatile-free), whereas olivine and pyroxene crystals are only found in the volcanic lithics (~ 65 wt% SiO_2 volatile-free). The El Escondido tuff cone is strongly eroded and Pela Huevos is a dome-like remnant in the SE sector. Because of this, along with the highly vegetated tropical zone where the volcanoes are emplaced as well as difficult political issues in the region, the edifices were not recognized until recently; this is why the younger cone was named "El Escondido" (which means "The Hidden"). These eruptions evidence that recent volcanism has occurred in a zone of the Central Cordillera that has been considered as non-volcanogenic in recent studies.

Keywords Samaná monogenetic volcanic field · Flat slab volcanism · Pre-existent eroded volcano · Silicic monogenetic volcanism · Recently discovered volcanoes

Introduction

Monogenetic volcanoes are small structures (volume < 1 km^3) that are formed by a single effusive and/or explosive eruption within a defined period of time (Kereszturi and Németh 2012; De Silva and Lindsay 2015) and can occur in any tectonic setting (Németh 2010). They are often grouped into monogenetic volcanic fields (Németh 2010; Cañón-Tapia 2016). Eruptions of monogenetic volcanoes are related to the rise of small magma batches (Németh 2010; Martí et al. 2016; Smith and Németh 2017). In general, these magma batches rapidly ascend to the surface through simple conduit systems, usually with little interaction with crustal rocks during ascent (Németh 2010). This is why, typically, monogenetic volcanoes are formed by relatively primitive magmas (Valentine and Greeg 2008; McGee and Smith 2016; Smith and Németh 2017). However, a few monogenetic volcanoes have erupted evolved magmas, suggesting some degree of stagnation in the crust (e.g., Borrero et al. 2017; Smith and Németh 2017; Murcia et al. 2019).

Editorial responsibility: P-S. Ross

✉ L. Sánchez-Torres
lsancheztorres15@gmail.com

1 Instituto de Investigaciones en Estratigrafía (IIES), Universidad de Caldas, Manizales, Colombia

2 Maestría en Ciencias de la Tierra, Universidad de Caldas, Manizales, Colombia

3 Programa de Geología, Universidad de Caldas, Manizales, Colombia

4 Departamento de Ciencias Geológicas, Universidad de Caldas, Manizales, Colombia

5 Grupo de Investigación en Estratigrafía y Vulcanología, GIEV Cumanday, Manizales, Colombia

6 Posgrado en Ciencias de la Tierra, Universidad Nacional Autónoma de México, México City, Mexico

El Escondido and Pela Huevos are dacitic monogenetic volcanoes located on the eastern flank of the Central Cordillera of Colombia, in the Selva de Florencia Natural National Park, 75 km NE of Manizales and 144 km NW of Bogotá, Colombia (Fig. 1a, b). The volcanoes are part of the Samaná monogenetic volcanic field (SMVF) (Borrero et al. 2017; Murcia et al. 2019) in the northern part of the San Diego – Cerro Machín Volcano Tectonic Province (Fig. 1b, c). El Escondido was recently discovered by the Colombian Geological Survey (Monsalve 2015; Monsalve and Arcila 2016) and defined as a pyroclastic-dome ring complex structure (Monsalve and Rueda 2015; Monsalve et al. 2019). This original definition included the Pela Huevos volcano as a dome being part of the El Escondido volcano. In that work, eruptive products were described as andesitic and dacitic in composition and at least two eruptions were reported by Monsalve et al. (2019): one at 36,030 ± 380 years BP and the other one at 33,550 ± 280 years BP. However, Sánchez-Torres (2017) and Toro and Delgado (2018) highlighted the strongly eroded character of El Escondido and Pela Huevos and based on field relations, proposed that the Pela Huevos dome was actually an older volcano affected by the El Escondido eruption. Recently, Rueda-Gutiérrez (2019) reported a 153.7 ± 38.2 ka $^{40}Ar/^{39}Ar$ age for the Pela Huevos dome.

This study focuses on the definition and distribution of the volcaniclastic deposits associated with El Escondido volcano. It also characterizes the composition of El Escondido and Pela Huevos volcanoes, based on petrography and whole-rock

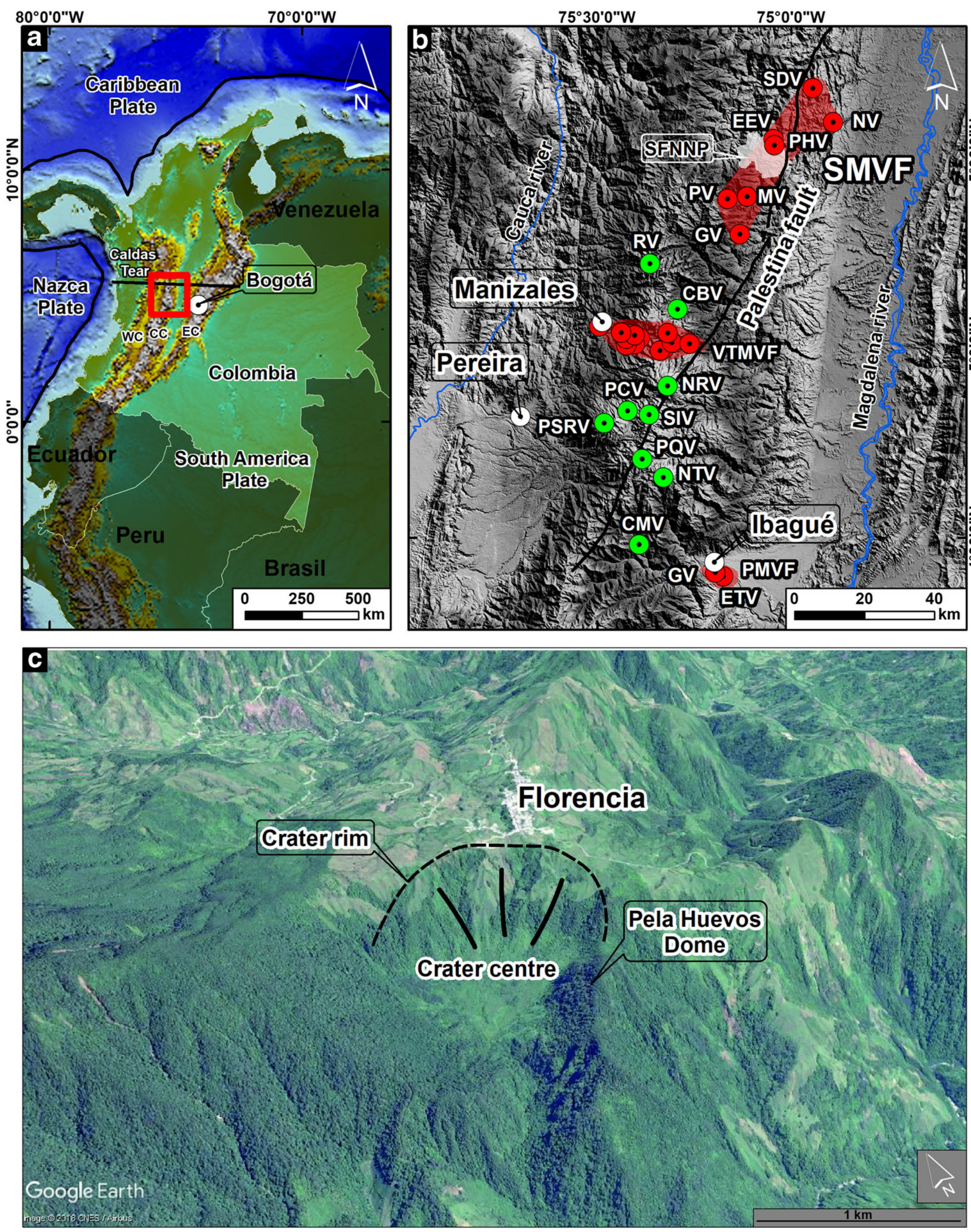

Fig. 1 Location maps. **a** Study site in Colombia. **b** San Diego – Cerro Machín Volcano Tectonic Province. Green dots are polygenetic volcanoes whereas red dots are monogenetic volcanoes. **c** Image of El Escondido and Pela Huevos volcanoes (taken from Google Earth; Map data: Image © CNES / Airbus). WC, West Cordillera; CC, Central Cordillera; EC, East Cordillera; SDV, San Diego volcano; NV, Norcasia volcano; EEV, El Escondido volcano; PHV, Pela Huevos volcano; MV, Morrón volcano; PV, Piamonte volcano; GV at north, Guadalupe volcano; RV, Romeral volcano; CBV, Cerro Bravo volcano; NRV, Nevado del Ruiz volcano; SIV, Nevado Santa Isabel volcano; PCV, Paramillo del Cisne volcano; PSRV, Paramillo de Santa Rosa volcano; PQV, Paramillo del Quindío volcano; NTV, Nevado del Tolima volcano; CMV, Cerro Machín volcano; GV at south, Guacharacos volcano; ETV, El Tabor volcano; SMVF, Samaná Monogenetic Volcanic Field; VTMVF, Villamaría-Termales Monogenetic Volcanic Field; PMVF, Pijaos Monogenetic Volcanic Field; SFNNP, Selva de Florencia Natural National Park

geochemistry. We also present new radiocarbon analyses of the El Escondido products. The results are integrated to (1) prove that volcanism is not uncommon in the region, (2) define the eruptive history in the area, and (3) highlight that this zone of the Colombian Andes, where a flat slab has been defined (Wagner et al. 2017), has produced recent volcanism. This information should be also useful for hazard evaluation in the region, considering that similar future eruptions cannot be ruled out in the monogenetic field.

Regional geological setting

El Escondido and Pela Huevos volcanoes are located in the Central Cordillera of Colombia, a long mountainous range where most of the volcanism occurs as a result of a subduction tectonic setting (Fig. 1a). The tectonic configuration of NW South America is dominated by three main lithospheric plates: the oceanic Nazca and Caribbean plates, and the continental South American plate (Taboada et al. 2000; Cediel et al. 2003; Cortés et al. 2005). The subduction of the Nazca and Caribbean plates is separated at 5.5°N forming two different Wadati-Benioff Zones: one associated with a flat, supposedly non-volcanogenic subduction to the north and another one associated with a "normal," volcanogenic subduction to the south (Vargas and Mann 2013; Idárraga-García et al. 2016; Syracuse et al. 2016; Wagner et al. 2017). This linear zone separating two different subduction angles responds to a lithospheric weakness; this is called the Caldas Tear mega suture (Vargas and Mann 2013) and is linked to the prolongation of the Sandra Ridge (Lonsdale 2005). Nonetheless, young volcanism (San Diego maar erupted 20 ky ago; Borrero et al. 2017) has now been found in the northern zone (cf. Murcia et al. 2019). El Escondido and Pela Huevos volcanoes are part of this volcanism.

The basement in the El Escondido area is composed of Triassic (Villagómez et al. 2011) or Upper Jurassic (Blanco-Quintero et al. 2014) metamorphic rocks of the Cajamarca Complex (Maya and González 1995; Maya 2001) and Lower Cretaceous rocks of the Samaná Igneous Complex (González 1990). These units are separated by the Palestina fault (Gómez-Tapias et al. 2015). In the study area, the Eocene Florencia Stock (54.9 ± 1.9 Ma: González 1990; 54.6 ± 4.4 Ma: Rueda-Gutiérrez 2019) intrudes the Cajamarca Complex (Fig. 2). This stock is composed of quartz diorite and biotite tonalite (González 1990). In the zone, there are also a series of Neogene plutonic bodies, which are dioritic to tonalitic in composition (Gómez-Tapias et al. 2015; Rueda-Gutiérrez 2019). Both El Escondido and Pela Huevos volcanoes are found overlying the Pleistocene Tefra amarilla (Yellow Tephra) unit that corresponds to an unmapped pyroclastic sequence with horizons of ash with altered lapilli-sized pumice fragments and bi-pyramidal quartz crystal fragments (Borrero et al. 2017).

Structurally, the studied volcanoes are in the area of influence of the Palestina fault, which has a right-lateral movement with a N30°E direction; this disposition is interpreted as the result of the oblique collision of the oceanic crust with the continental crust during the Late Cretaceous (Feininger 1970; Cortés et al. 2005). This fault coincides with the alignment of the volcanic centers on the axis of the Central Cordillera (Borrero et al. 2017) (Fig. 1b).

El Escondido and Pela Huevos volcanoes: general features

El Escondido (5° 31′ 00″ N, 75° 02′15″ W, 1500 m above sea level, a.s.l.) is a strongly eroded and heavily vegetated tuff cone. It occurs in a mountainous region with steep relief and pronounced valleys. The northern and eastern sectors of the edifice are partly preserved, whereas the southern and western parts have been eroded (Figs. 1c and 2). The volcano has a 1.50×1.25 km wide and 250 m deep crater, with the highest rim point at 1633 m a.s.l. The volcaniclastic deposits of the volcano are mainly preserved N and E of the crater, where the town of Florencia (3000 inhabitants) is settled. To the SE, a small dome-like hill represents the remnant of the Pela Huevos volcano (5° 30′ 48.14″ N, 75° 02′ 37.06″ W, 1500 m a.s.l) (Fig. 1c). Thermal springs are found in the area, presumably due to magmatic heat at depth (cf. Rueda-Gutiérrez 2019).

Methodology

Stratigraphic, compositional, textural, and radiocarbon analyses are used to study the volcanic products in the area. Field work was carried out to define the stratigraphy of the El Escondido deposits and to collect samples of each defined unit. Characteristics such as fabric, sorting, granulometry, color, and sedimentary structures of the deposits were evaluated in the field (following Murcia et al. 2013). We apply the term matrix to fragments less than 2 mm in diameter. After sieving, the 0 ϕ (1–2 mm) size fraction of each unit was studied under a binocular microscope: approximately 300 particles were counted for componentry. The main types of fragments present at El Escondido were studied through thin sections and major element geochemistry. Specifically, two pumice fragments and two block-sized lithic volcanic fragments were analyzed. Crystal size was defined following González (2008), where phenocrysts are > 0.50 mm and microphenocrysts range between 0.05 and 0.50 mm; microlites (< 0.05 mm) are part of the groundmass. Point counting of thin sections (groundmass vs vesicles vs crystals) was done with a

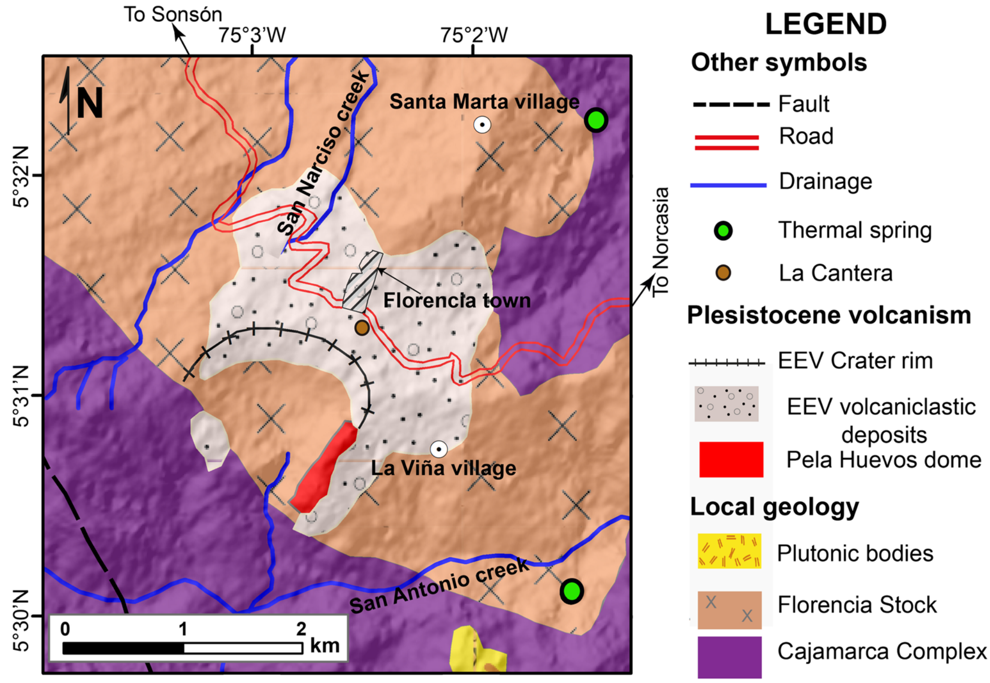

Fig. 2 Geological map of El Escondido volcano area. Modified from Gómez-Tapias et al. (2015)

petrographic microscope at the Instituto de Investigaciones en Estratigrafía (IIES) at the Universidad de Caldas, Manizales, Colombia. Chemical analyses were performed through ICP-OES in the ActLab and SGS commercial laboratories in Colombia. Vesicularity was determined for 30 pumice fragments (> 2 cm) per stratigraphic unit following the vesicularity index of Houghton and Wilson (1989) and the methodology of Gardner et al. (1996). Morphology of pumice fragments was studied on 20, 125–500 μm pumice fragments using a QUANTA 250 Scanning Electron Microscope (SEM) at IIES; thus, high-resolution images of the vesicles and their walls were obtained. Finally, two samples of charcoal found in El Escondido deposits were dated using the ^{14}C radiocarbon method at Centre d'Études Nordiques, Université Laval, Quebéc, Canada. Ages were calibrated using the IntCal13 curve (Reimer et al. 2013).

Results

Stratigraphy, sedimentary characteristics, and distribution of volcaniclastic deposits

The deposits of El Escondido volcano are distributed towards the N and E sides of the emission center (Fig. 2). The volcaniclastic deposits are mostly altered, strongly affected by erosion and poorly consolidated. Based on unconformities (cf. Martí et al. 2018), nine stratigraphic units, with clear lower and upper limits, were determined: U0 to U8 from the base to the top (Figs. 3 and 4). Units U0 to U7 were defined at a single location named "La Cantera" at the outskirts of Florencia town (~ 150 m from the crater rim; Fig. 2), and these could be followed around the volcano. An additional unit (U8) was observed only at the rim of the crater.

Unit 0: This unit has an exposed thickness of 68 cm, although the base was not observed. It is formed by a clast-supported deposit, which is well sorted, poorly consolidated, grayish in color, with sub-rounded and sub-angular fragments dominantly sized from 3 mm (fine lapilli) to 4 cm (coarse lapilli) (Fig. 5a). The > 2 mm fragments (70 vol%) correspond to pumice (90 vol%) and plutonic lithics (10 vol%) (Fig. 5b). The ashy matrix makes up 30 vol% of the deposits and contains pumice fragments (83 vol%), plutonic and metamorphic lithics (15 vol%) and volcanic lithics (2 vol%) (Fig. 3).

Unit 1: This unit has a thickness of 25 cm. It is formed by a clast-supported deposit. The deposit is well sorted, dark gray in color, with angular and sub-angular fragments dominantly sized from 1 cm (medium lapilli) to 6 cm (coarse lapilli) (Fig. 5c, d). The > 2 mm fragments (80 vol%) correspond to dense volcanic lithics (85 vol%), pumice (10 vol%), and plutonic lithics (5 vol%). The matrix (20 vol%) is formed by dense volcanic lithics (65 vol%), pumice (28 vol%), and plutonic lithics (7 vol%) (Fig. 3).

Unit 2: This unit has a thickness of 4.4 m. It is similar to Unit 0 and is formed by a clast-supported deposit (Fig. 5e). The deposit is poorly sorted, poorly consolidated, grayish in color, with angular to sub-angular fragments dominantly sized from 5 mm (fine lapilli) to 30 cm (fine-blocks). The > 2 mm fragments (85 vol%) correspond to pumice (70 vol%), plutonic lithics (20 vol%), and dense volcanic lithics (10 vol%) (Fig. 5f). The matrix (15 vol%) is formed by pumice fragments (77 vol%), plutonic and metamorphic lithics (13.5 vol%) and dense volcanic lithics (9.5 vol%) (Fig. 3). In the upper

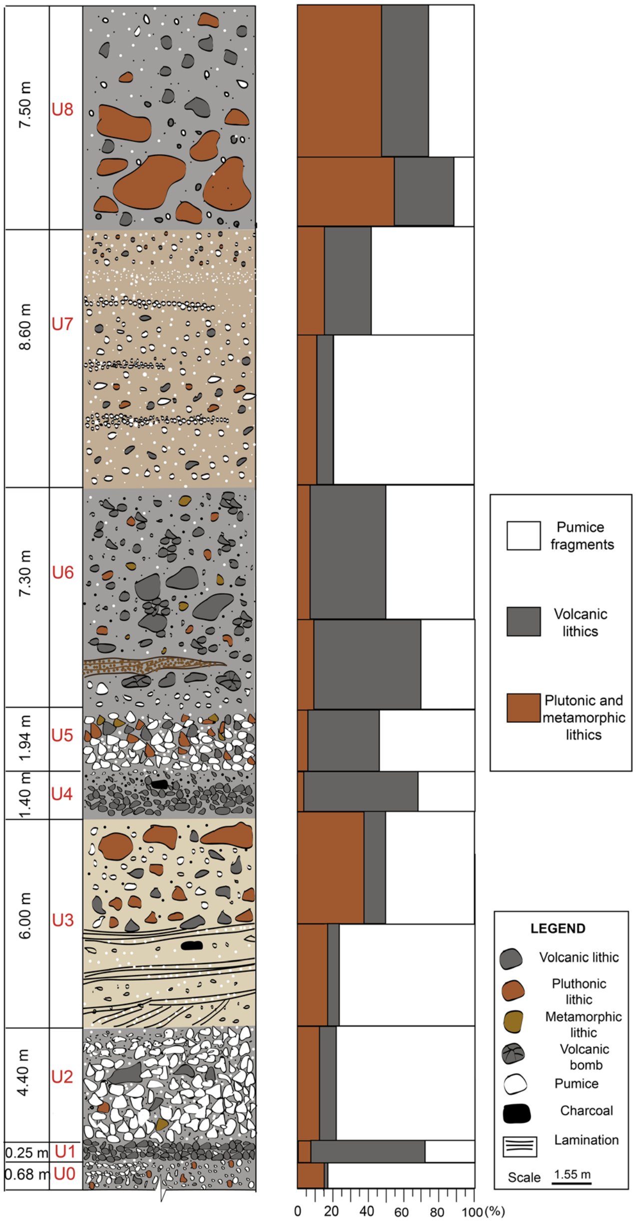

Fig. 3 Stratigraphic column and matrix componentry variation diagram of the stratigraphic units defined for El Escondido volcano

part of the unit, two thin grayish lenticular layers of finer material of the same composition were observed. In the middle part of the unit, block-sized volcanic fragments are sporadically present.

Unit 3: This 6.0-m-thick unit has two distinct matrix-supported portions. The lower half is finer-grained and internally stratified (plane-parallel to low angle cross-lamination) (Fig. 5g), whereas the upper half is coarser grained and internally structureless.

In more detail, the lower half is well sorted, brownish in color, with sub-rounded fragments with an average size of 2 mm (very coarse ash). The > 2 mm fragments (30 vol%) correspond to pumice (85 vol%), dense volcanic lithics (10 vol%), and plutonic lithics (5 vol%). The matrix (70 vol%) is formed by pumice (76 vol%), plutonic lithics (18 vol%), and dense volcanic lithics (6 vol%).

The upper half is poorly sorted, hardened, brownish in color, with sub-rounded fragments dominantly sized from 1 cm (medium lapilli) to 60 cm (medium-block) (Fig. 5h). The > 2 mm fragments (40 vol%) correspond to pumice (60 vol%), plutonic lithics (25 vol%), dense volcanic lithics (10 vol%), and metamorphic lithics (5 vol%). The largest fragments correspond to plutonic rocks. The matrix (60 vol%) is formed by pumice (50 vol%), plutonic and metamorphic lithics (37 vol%), and dense volcanic lithics (13 vol%) (Fig. 3). Within the lower deposits, charcoal was found (Fig. 5i).

Unit 4: This 1.4-m-thick unit is very similar to Unit 1. It consists of a normally graded, clast-supported, well sorted, moderately consolidated, dark gray deposit. The angular to sub-angular fragments are dominantly sized from 1 cm (medium lapilli) to 12 cm (fine-block) (Fig. 5j). The > 2 mm fragments (70 vol%) correspond to dense volcanic lithics (85 vol%), plutonic lithics (5 vol%), and pumice (10 vol%). The matrix (30 vol%) is formed by dense volcanic lithics (64 vol%), pumice (33 vol%), and plutonic lithics (3 vol%) (Fig. 3). Within the deposit, charcoal was also found (Fig. 5k).

Unit 5: This 1.9-m-thick unit is similar to units 0 and 2. It is formed by a clast-supported deposit. The deposit is poorly sorted, moderately consolidated, grayish in color, with angular and sub-angular fragments dominantly sized from 2 cm (medium lapilli) to 16 cm (fine-block) (Fig. 5l). The > 2 mm fragments (75 vol%) correspond to pumice (75 vol%), dense

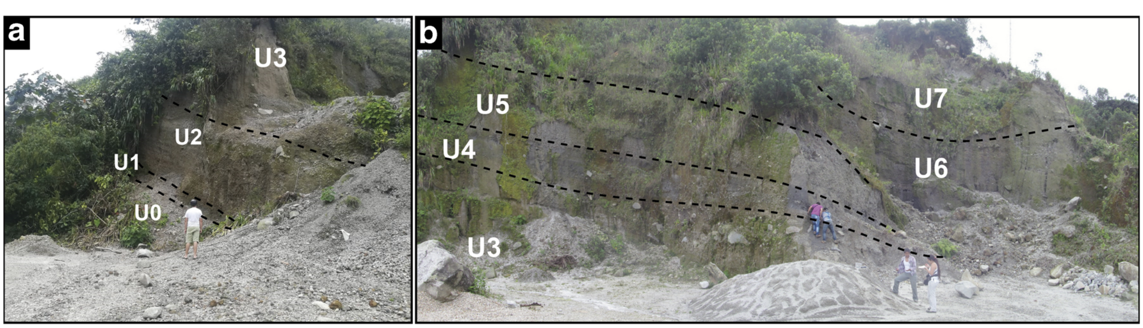

Fig. 4 General stratigraphy of the deposits of El Escondido volcano. **a** Lower units; outcrop is 7 m high. **b** Upper units; outcrop is 10 m high

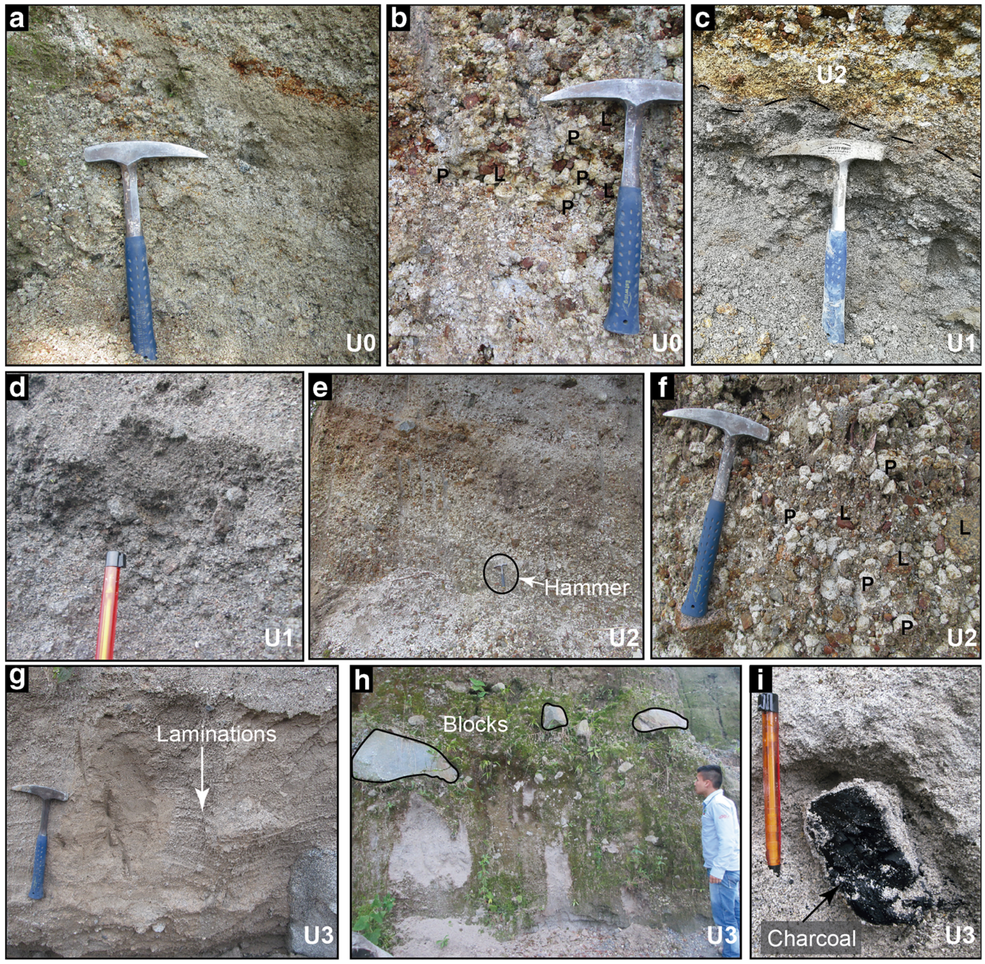

Fig. 5 Main characteristics of some stratigraphic units. **a** Pumiceous deposits of U0. **b** Pumice and lithics fragments of U0. **c**, **d** Volcanic lithic-rich deposits of U1. **e** Pumiceous deposits of U2. **f** Pumice and lithics fragments of U2. **g** Matrix-supported fabric with laminations in U3. **h** Matrix-supported fabric with block-sized fragments in U3. **i** Charcoal fragment inside U3. The hammer is 33 cm long and the pen is 14 cm long. **j** Volcanic lithic-rich deposits of U4. **k** Charcoal fragment inside U4. **l** Pumiceous deposits of U5. **m** Volcanic lithic-rich deposits of U6. **n** Layer present in the middle part of U6; this layer has accretionary lapilli. **o** Fragments of bread-crust bombs at the base of U6. **p**, **q** Pumiceous deposits of U7. **r** Block-sized sub-rounded fragments inside U8. The hand lens is 2 cm in external diameter

volcanic lithics (15 vol%), and plutonic lithics (10 vol%). The matrix (25 vol%) is formed by pumice (54 vol%), dense volcanic lithics (40 vol%), and plutonic and metamorphic lithics (6 vol%) (Fig. 3).

Unit 6: This 7.3-m-thick unit, similar to units 1 and 4, is formed by a clast-supported deposit. The deposit is poorly sorted, friable, grayish to brownish in color, with angular and sub-angular fragments dominantly sized from 2 cm (coarse lapilli) to 30 cm (medium-block) (Fig. 5m). The > 2 mm fragments (90 vol%) correspond to dense volcanic lithics (50 vol%), plutonic lithics (15 vol%), pumice (30 vol%), and metamorphic lithics (5 vol%). The matrix (10 vol%) is formed by dense volcanic lithics (66 vol%), pumice (25 vol%), and plutonic and metamorphic lithics (9 vol%) at the base; and dense volcanic lithics (49 vol%), pumice (45 vol%), and plutonic and metamorphic lithics (6 vol%) at the top (Fig. 3). Within the lower third of the unit, a 37-cm-thick lens with plane-parallel laminations and abundant accretionary lapilli was observed (Figs. 3 and 5n). At the base of Unit 6, bread-crust bombs up to 50 cm in diameter appear (Fig. 5o).

Unit 7: This 8.6-m-thick unit is very similar to units 0, 2, and 5, and it is formed by a matrix-supported deposit. The deposit is well sorted, poorly consolidated, grayish in color, with sub-rounded and sub-angular fragments sized mostly from 2 to 6 cm (coarse lapilli). The > 2 mm fragments (45 vol%) correspond to pumice (75 vol%), dense volcanic lithics (15 vol%), and plutonic and metamorphic lithics (10 vol%). The matrix (55 vol%) is formed by pumice (80 vol%), plutonic and metamorphic lithics (11 vol%), and dense volcanic lithics (9 vol%) at the base. The matrix in the top part consists of pumice (59 vol%), dense volcanic lithics (25 vol%), and plutonic and metamorphic lithics (17 vol%) (Fig. 3). In the middle of the unit, lenses of finer pumice fragments can be observed (Fig. 5p, q).

Unit 8: This 7.5-m-thick unit is formed by a matrix-supported deposit. The deposit is poorly sorted, hardened, brownish in color with yellowish shades, with rounded and sub-rounded fragments dominantly sized from 10 cm (fine-block) to 2 m. The > 2 mm fragments (30 vol%) correspond to plutonic lithics (60 vol%), dense volcanic lithics (20 vol%), metamorphic lithics (10 vol%), and pumice fragments (10 vol%) (Fig. 5r). The matrix (70 vol%) has been quantified in two samples. In the lower part of the unit, the matrix is formed by plutonic and metamorphic lithics (55 vol%), dense volcanic lithics (34 vol%), and pumice (11 vol%). In the top, it

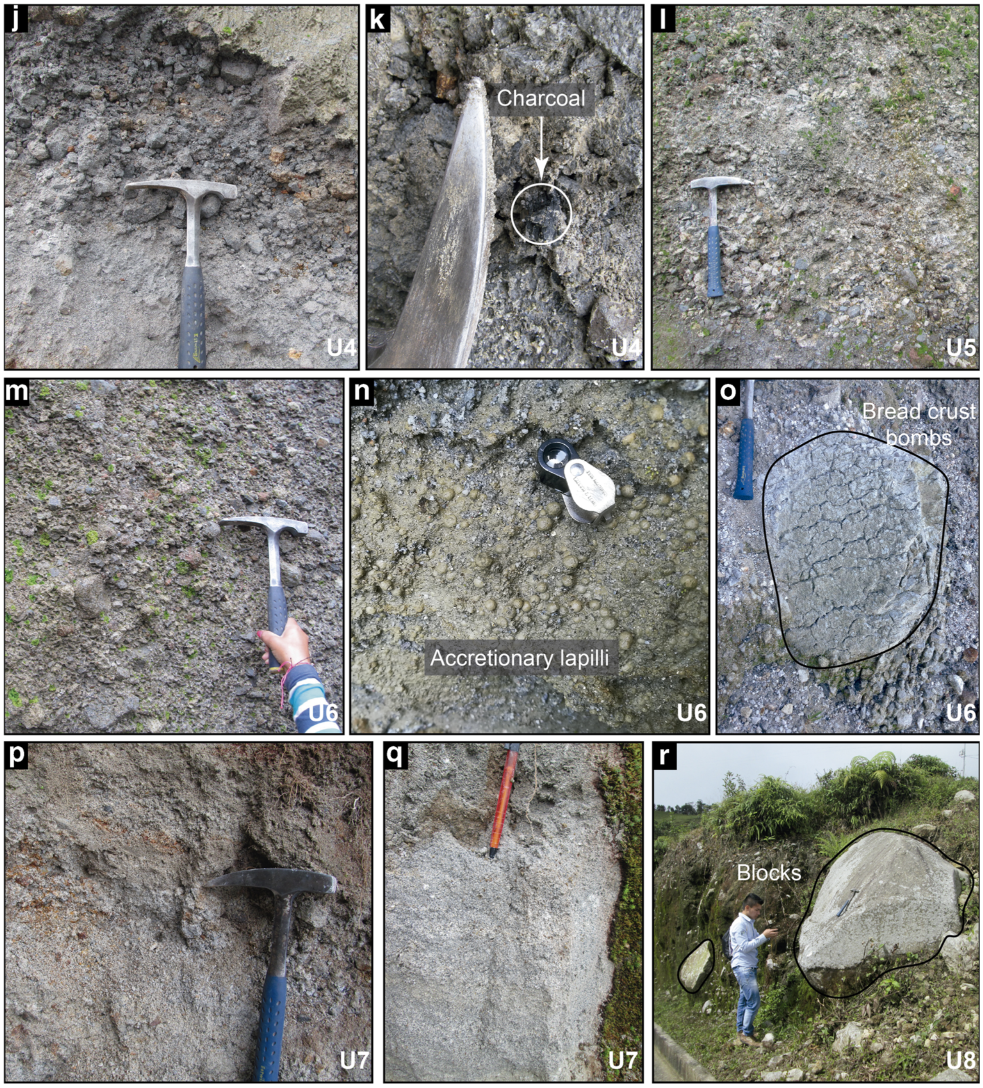

Fig. 5 (continued)

is formed by pumice (25 vol%), plutonic and metamorphic lithics (47 vol%), and dense volcanic lithics (28 vol%) (Fig. 3).

Petrography and geochemistry

Four rock samples were petrographically and geochemically analyzed: two pumice fragments from U2, a dense volcanic lithic from U4, and a dense sample from the Pela Huevos volcano.

The pumice fragments are hypohyaline porphyritic with a glassy groundmass, whereas the dense rocks are hypocrystalline porphyritic with a glassy groundmass with microlites. Plagioclase (10–28 vol%) and amphibole (6–16 vol%) are ubiquitous in all four samples and occur as phenocrysts and microphenocrysts (Fig. 6a, b, c). Biotite (3–7 vol%) and quartz (1–2 vol%) occur as microphenocrysts in the pumice only (Fig. 6d, e). Pyroxene (0–2 vol%) and olivine (1 vol%) are present as microphenocrysts in the dense samples (Fig. 6f, g, h) (Table 1). All rocks display low percentages (< 1 vol%) of oxide minerals. In the pumice, petrography also evidences sieve texture in plagioclase, and glomeroporphyritic texture formed by plagioclase and amphibole, or by a mix between plagioclase, amphibole, and quartz. In the dense volcanic rocks, sieve texture in plagioclase is characteristic; glomeroporphyritic texture also appears and is formed by plagioclase, amphibole, and pyroxene, or by a mix between amphibole and plagioclase, or amphibole and olivine. Seriate and trachytic textures are also formed by the plagioclase.

Geochemically, all four samples display a dacitic composition according to the TAS diagram (Fig. 7a) (Le Bas et al. 1986), although the pumice fragments clearly are more silicic (SiO_2 ~ 70 wt% on an anhydrous basis) in comparison with the dense volcanic rocks (SiO_2 ~ 65 wt% on an anhydrous basis). All of the samples are located in the calc-alkaline field

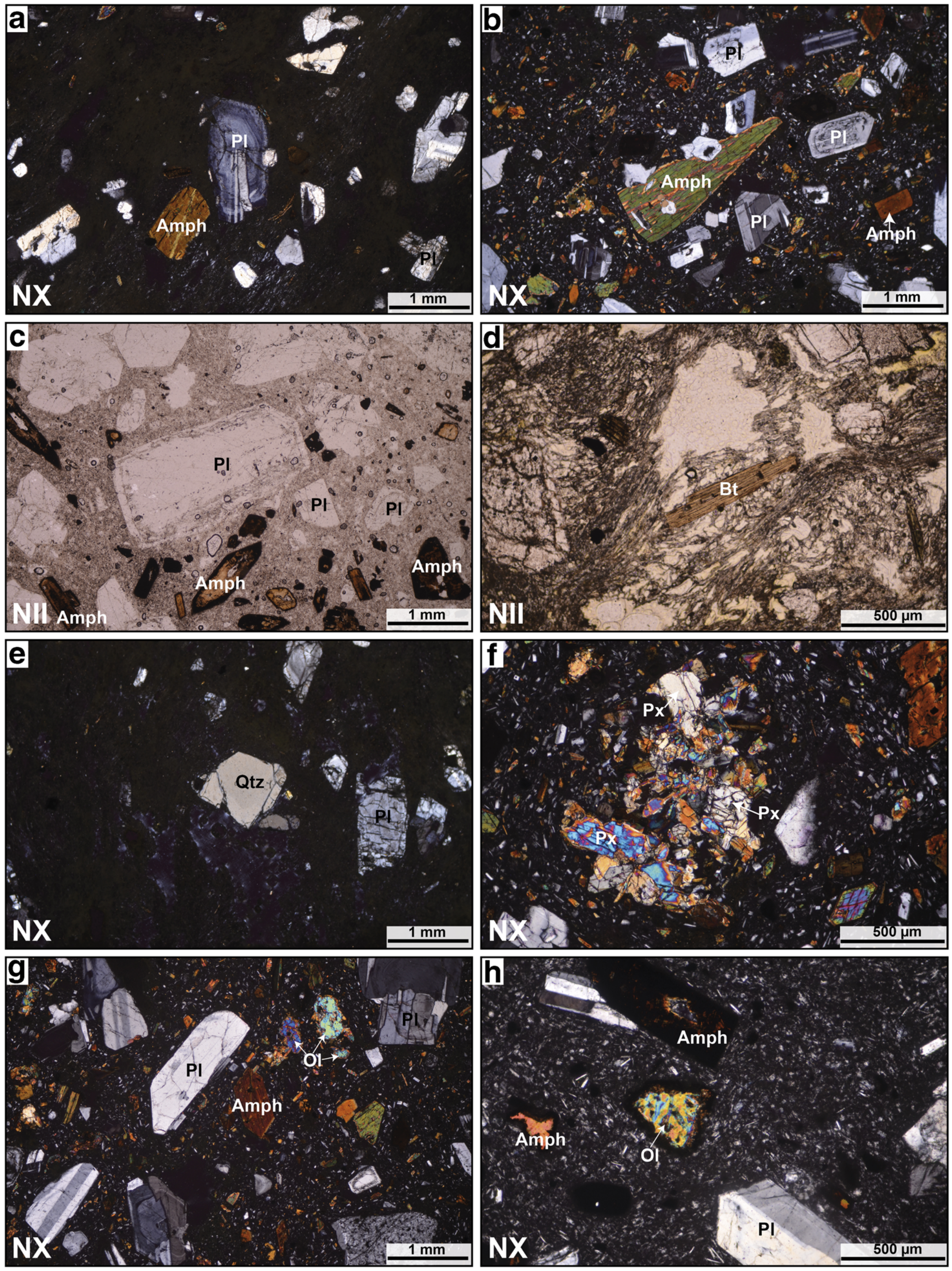

Fig. 6 Photomicrographs of fragments within the El Escondido (EE) volcaniclastic deposits and from the Pela Huevos volcano. **a** Plagioclase and amphibole phenocrysts in the EE pumice fragments. **b** Plagioclase and amphibole phenocrysts and microphenocrysts in the dense volcanic lithics at EE. **c** Plagioclase and amphibole phenocrysts and microphenocrysts in the sample from Pela Huevos. **d** Biotite microphenocrysts in pumice fragments at EE. **e** Quartz microphenocrysts in pumice fragments at EE. **f** Pyroxene microphenocrysts in dense volcanic lithics at EE. **g** Olivine microphenocrysts in dense volcanic lithics at EE. **h** Olivine microphenocrysts in the Pela Huevos sample. Mineral abbreviations are taken from Kretz (1983): Amphibole (Amph), Biotite (Bt), Olivine (Ol), Plagioclase (Pl), Pyroxene (Px), Quartz (Qtz)

Table 1 Percentages of crystals, vesicles, and groundmass obtained in the petrographic point-counting analysis

Sample	% groundmass	% vesicles	% crystals					
			Pl	Amph	Bt	Qz	Px	Ol
Pumice 1	54.9	22	10.7	7.8	3.3	1.4	0	0
Pumice 2	37.8	37.1	9.8	6.3	7	2.1	0	0
Lithic	59.2	0	22	15.1	0	0	1.6	1.3
Dome	55.3	0	27.9	16.1	0	0	0	0.6

on the AFM diagram (Fig. 7b) (Irvine and Baragar 1971) and in the medium-K field in the SiO_2 vs K_2O diagram (Fig. 7c) (Peccerillo and Taylor 1976) (Table 2).

Textural characteristics

Vesicularity analysis in pumice fragments were performed for U2 and U5 as they were the units where pumice fragments >2 cm were found. The results indicate a somewhat heterogeneous vesicularity. It ranges from 56 to 81 vol%, varying from moderately to extremely vesicular,

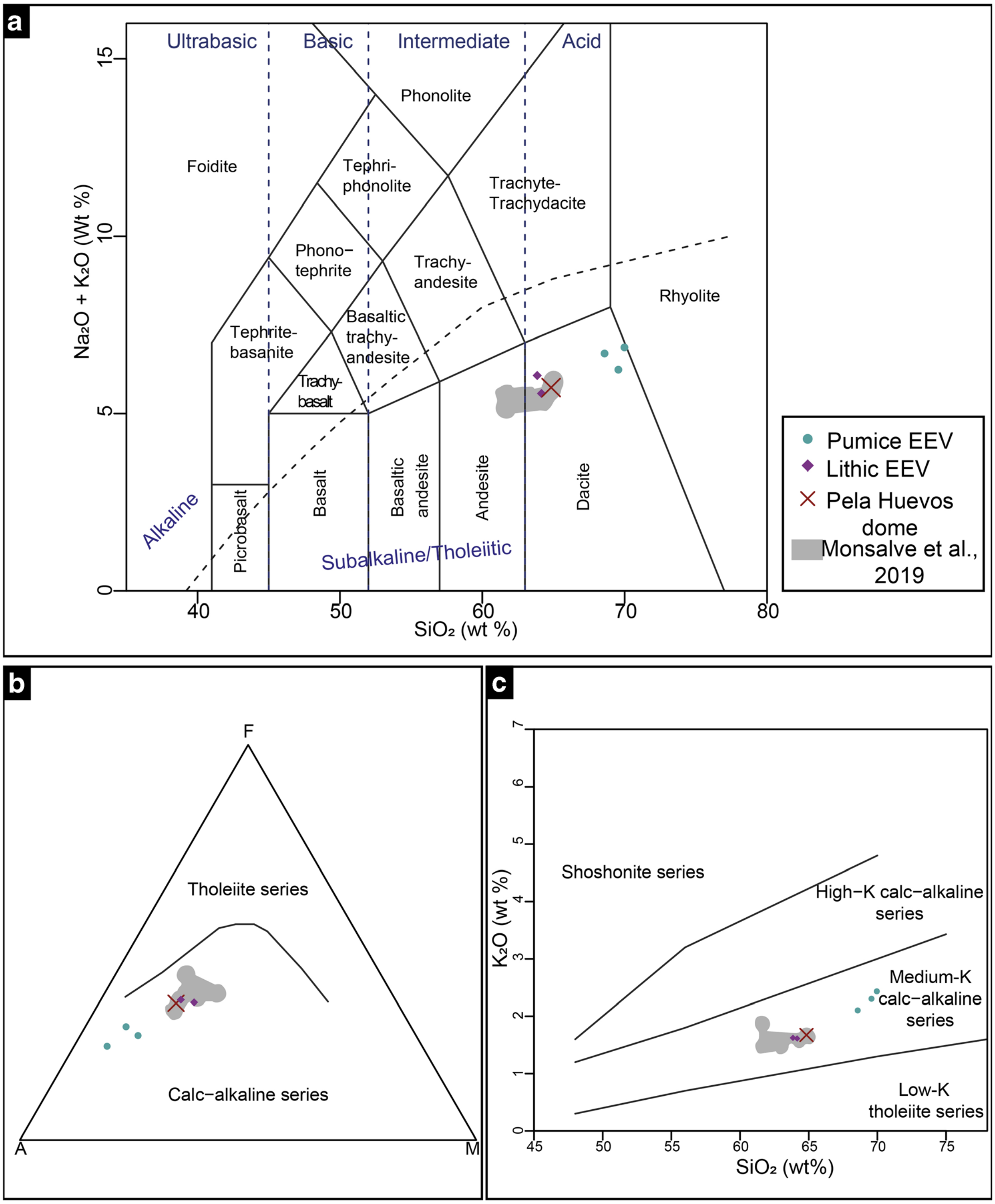

Fig. 7 Geochemical classification diagrams. Four samples were analyzed, including two samples at both laboratories, for a total of six data points (Table 2). **a** TAS diagram (Le Bas et al. 1986). **b** AFM diagram (Irvine and Baragar 1971). **c** K_2O vs SiO_2 diagram (Peccerillo and Taylor 1976 modified by Le Maitre et al. 2002)

although almost all clasts are highly vesicular (Fig. 8). The average vesicularity is 73.5 vol% for U2, and 65.3 vol% for U5.

Morphological analysis of pumice fragments was performed for U0, U2, U5, U6, and U7 as they were the units where pumice fragments between 125 and 500 μm were found. The fragments exhibit a wide spectrum of vesicle shapes and sizes; vesicles range from spherical and homogeneous (U2, U5, and U6; Fig. 9a) to elongated and heterogeneous (U0 and U5; Fig. 9b). Tube pumice is seen in U2 and U5 (Fig. 9c). Fragments exhibit microstructures such as cracks (U0, U6, and U7; Fig. 9d), glass dehydration cracks (U0; Fig. 9e), and spongy microtexture (U6 and U7; Fig. 9F).

Table 2 Major elements in the analyzed samples

Sample	*Pumice 1	°Pumice 1	°Pumice 2	*Litihic	°Lithic	*Dome
wt%						
SiO2	66.47	67.11	66.51	63.62	62.87	63.89
Al2O3	15.11	15.73	15.42	16.16	16.21	17.15
Fe2O3(T)	2.88	3.34	2.48	4.81	5.02	4.48
MnO	0.13	0.13	0.13	0.11	0.12	0.12
MgO	1.24	0.94	0.71	2.58	2.23	1.97
CaO	3.34	3.64	2.98	5.70	5.35	4.68
Na2O	3.76	4.49	4.19	3.92	4.38	4.00
K2O	2.2	2.06	2.32	1.60	1.60	1.65
TiO2	0.26	0.29	0.22	0.49	0.47	0.46
P2O5	0.16	0.13	0.12	0.17	0.20	0.14
LOI	3.13	2.2	3.69	1.22	1.02	1.18
Total	98.67	100.07	98.77	100.4	99.48	99.72

*Actlabs laboratory

°SGS laboratory

El Escondido volcano age

Charcoal fragments were collected in two units (U3 and U4; Fig. 5i, k). Radiocarbon dating of these fragments yielded ages of 34,060 ± 240 years BP (38,553 ± 596 years Cal. BP), and 33,230 ± 220 years BP (37,484 ± 798 years Cal. BP), respectively. These ages partly overlap (Table 3).

Discussion

Pela Huevos versus El Escondido

In the SMVF, two volcanoes have been studied in some detail so far: San Diego maar (Borrero et al. 2017) and El Escondido tuff cone (Monsalve et al. 2019; this study). In the area, however, other volcanic centers have been recently identified (e.g., Guadalupe, Piamonte, Morrón, and Norcasia volcanoes; SGC 2017; Borrero et al. 2017; Murcia et al. 2017, 2019).

Pela Huevos hill is the remnant of an older volcano (Sánchez-Torres 2017; Toro and Delgado 2018) as evidenced by field work (Pela Huevos-like lithics within the El Escondido deposits), petrography (Fig. 6), geochemistry (Fig. 7), and dating (Rueda-Gutiérrez 2019). Therefore, Pela Huevos is not part of the El Escondido eruptive history (cf. Monsalve et al. 2019). Instead, rock fragments from Pela Huevos were incorporated during the El Escondido eruption, and the volcano was partly destroyed by the El Escondido eruption. Overall, we found that the pumice fragments of El Escondido deposits are the juvenile clasts while the dense volcanic lithics are the accessory fragments (sensu Murcia et al. 2013).

How many eruptions?

Paleosols are absent in the El Escondido volcaniclastic deposits. Unconformities are mostly represented by granulometric changes and/or contacts between different types of volcaniclastic deposits as well as remobilization or minor erosion surfaces typical between these deposits. Therefore, unconformities can be considered as minor (cf. Martí et al. 2018). Minor unconformities can appear between successive eruptions (inter-eruption) but also between different pulses (intra-eruption). As mentioned above, radiocarbon ages obtained from charcoal material in U3 and U4 yielded partly overlapping ages, which is compatible with the idea that El Escondido was formed by a single eruption around 38,000 years ago. This contradicts the interpretation by Monsalve et al. (2019) who invoke at least two eruptions for El Escondido volcano based on an older date (40,667 ± 807 years Cal. BP) for their unit UL, which is our U3. We obtained a younger age (38,553 ± 596 years CalBP) for the same unit, and the source of the different ages is not clear. Nevertheless, the bulk of the evidence currently points to a single monogenetic eruption at El Escondido.

Origin of the El Escondido volcaniclastic units

Units 0, 2, 5, and 7 are coarse, clast-supported, well-to-poorly sorted, poorly-to-moderately consolidated, pumice-rich deposits. They are pyroclastic in origin, but their mode of emplacement is not clear. Possibilities include proximal fallout and pumiceous pyroclastic density currents, a.k.a. ignimbrites. The latter have been reported in other monogenetic eruptions such as in La Garrotxa Volcanic Field in Spain (Martí et al. 2017), and recently in Colombia, in the Paipa Volcanic Field (Suárez 2016).

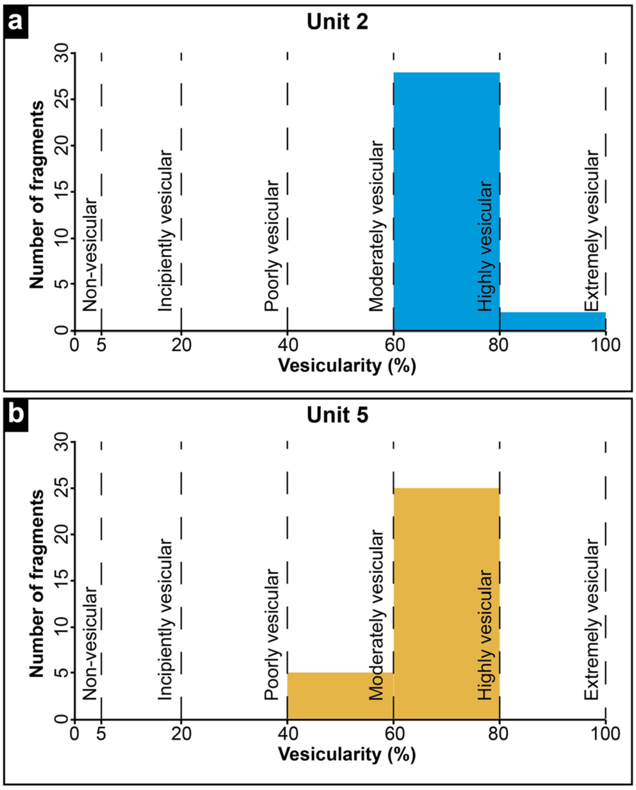

Fig. 8 Vesicularity histograms of pumice fragments. **a** U2. **b** U5. The vesicularity ranges are taken from Houghton and Wilson (1989)

Unit 1, unit 4, and most of unit 6 are coarse, clast-supported, well-to-poorly sorted, sometimes normally graded, moderately consolidated to friable, lithic-rich deposits. Again, they are thought to be pyroclastic in origin, but their mode of emplacement is unclear. Possibilities include proximal fallout and lithic-rich pyroclastic density currents. The finer-grained lens within unit 6 has plane-parallel laminations and abundant accretionary lapilli, and is interpreted as the deposits of more dilute pyroclastic density currents, a.k.a. surges.

Units 3 and 8 are interpreted as lahar deposits which were formed during the eruption or, for unit 8, slightly after. Specifically, unit 8 and the upper half of unit 3 are thought to represent debris flow deposits based on the general lack of internal structure, the matrix-supported fabric, the poor sorting, the presence of large sub-rounded plutonic blocks, and the hardened character of the matrix. The lower part of unit 3 is interpreted as the deposit of a hyperconcentrated flow (a more dilute lahar) based on better sorting and the presence of sedimentary structures (Vallance and Iverson 2015).

Magma fragmentation

Two mechanisms have been defined for magma fragmentation: magmatic (Cashman and Scheu 2015) and phreatomagmatic (Zimanowski et al. 2015). To differentiate between these processes, different approaches can be investigated, as summarized by White and Valentine (2016), of which we consider three. The first is the vesicularity of juvenile fragments (Houghton and Wilson 1989; Cashman et al. 2000). High vesicularity (typically > 70 vol% for felsic magmas) suggests magmatic fragmentation, while lower vesicularity, and a broader range of vesicularities, suggests phreatomagmatic processes (Houghton and Wilson 1989). A second approach is the morphological characteristics of juvenile glass particles. Spongy textures are considered typical of magmatic fragmentation (Heiken 1972, 1974; Houghton and Wilson 1989; Cashman et al. 2000). A third criterion is the proportion of lithic clasts. A high abundance of lithic fragments from the basement could suggest phreatomagmatism (Morrissey et al. 2000; Zimanowski et al. 2015).

For El Escondido volcano, many depositional units are pumice-rich, and vesicularity values of the > 2 mm juvenile fragments are relatively high (62–82 vol% for U2 and 56–74 vol% for U5) and have narrow distributions (Fig. 8). This suggests extensive vesiculation and magmatic fragmentation. In terms of morphology characteristics, a magmatic fragmentation process is evidenced by the identified spongy textures (Hougthon and Wilson 1989; Cashman et al. 2000). However, the relatively large proportion of fragments from the basement in some units (e.g., up to 18 vol% in U2) evidences strong basement disruption (vent widening) in some phases of the eruption, perhaps associated with explosive magma-water interaction. Within unit 6, a thin subunit with accretionary lapilli and laminations might represent surges caused by phreatomagmatism (cf. Branney and Kokelaar 2002). The water associated with this process was stored in a confined aquifer within the fractured and foliated Cajamarca Complex (cf. Borrero et al. 2017).

Conclusions

The deposits of the 38 ka El Escondido volcano are distributed in an area of approximately 1.5 km around the crater, with a greater distribution to the north and much less to the south. This could be related to the high rate of erosion in the area, or simply to no deposition towards the south at the time of the eruption.

Compositional analysis reflects mineralogical and chemical differences between the juvenile pumice and the dense volcanic lithics in the El Escondido deposits. This, along with new geochronology data, demonstrates the existence of a previous volcano in the area, the ~ 154 ka Pela Huevos, in the SE sector of the El Escondido edifice. The accessory dense volcanic lithics

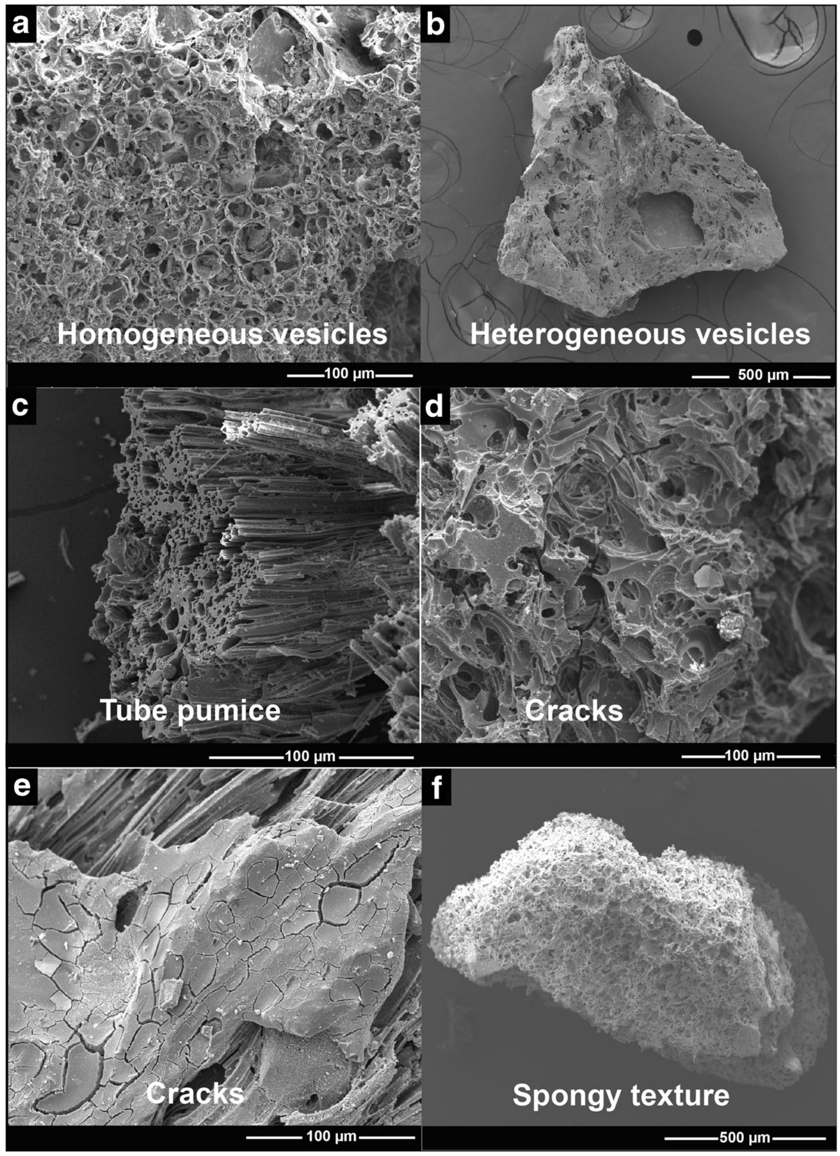

Fig. 9 Morphological and vesicle characteristics of pumice fragments observed by scanning electron microscope. **a** Homogenous vesicles (U2). **b** Heterogeneous vesicles (U0). **c** Tube pumice (U5). **d** Cracks (U7). **e** Glass dehydration cracks (U0). **f** Spongy texture (U7)

in the El Escondido volcaniclastic deposits were derived from Pela Huevos.

These volcanoes, as well as the previously defined San Diego maar (20 ka), prove that in NW South America, the flat subduction zone north of 5.5°N is volcanogenic, having generated the Samaná monogenetic volcanic field in Colombia. This volcanic field must be considered active, with hazard implications for the region, and adds a further tectonic setting to the global catalog of monogenetic volcanism.

Table 3 ^{14}C radiocarbon ages for El Escondido volcano

Unit	Code	Université Laval code	Pre-treatments	$F^{14}C$	±	$D^{14}C$ (‰)	±	^{14}C age (BP)	±	Calibrated age* (Cal. BP)	
4	VEE-01C	ULA-7683	HCl-NaOH-HCl	0.0160	0.0004	− 984.0	0.4	33,230	220	38,282–36,686	37,484 ± 798
3	VEE-02C	ULA-7684	HCl-NaOH-HCl	0.0144	0.0004	− 985.6	0.4	34,060	240	39,149–37,957	38,553 ± 596
^K	–	–	–	–	–	–	–	33,550	280	38,446–36,721	37,584 ± 863
^K	–	–	–	–	–	–	–	33,719	268	38,784–37,186	37,985 ± 799
^L	–	–	–	–	–	–	–	36,030	380	41,474–39,860	40,665 ± 805

*Calibrated age using the program OxCal 4.3. See website: https://c14.arch.ox.ac.uk/oxcal.html#program (OxCal online). Probability used to calibrate: 95.4%. Calibration curve used: IntCal13. ^Ages of Monsalve et al. (2019)

Acknowledgments This work was performed at the Instituto de Investigaciones en Estratigrafía (IIES), Universidad de Caldas. The Vicerrectoría de Investigaciones y Posgrados from the same university provided funds through the Semillero de Investigación en Vulcanología as part of the Grupo de Investigación en Estratigrafía y Vulcanología (GIEV) Cumanday. The Parque Natural Nacional Selva de Florencia supported the field work, while the Alcaldia de Samaná provided funds for the radiocarbon dating. Dario Pedrazzi, two anonymous reviewers, and associate editor P.-S. Ross made helpful suggestions on the manuscript.

References

Blanco-Quintero A, García-Casco L, Toro LM, Moreno M, Ruiz EC, Vinasco CJ, Cardona A, Lázaro C, Morata D (2014) Late Jurassic terrane collision in the northwestern margin of Gondwana (Cajamarca Complex, eastern flank of the Central Cordillera, Colombia). Int Geol Rev 56:1852–1872

Borrero C, Murcia H, Agustin-Flores J, Arboleda MT, Giraldo AM (2017) Pyroclastic deposits of San Diego maar, Central Colombia: an example of a silicic magma related monogenetic eruption in a hard substrate. In: Németh K, Carrasco-Núñez G, Gómez JJ, Smitih IEM (eds) Monogenetic volcanism, Geological society special publication, vol 446, pp 361–374

Branney MJ, Kokelaar BP (2002) Pyroclastic density currents and the sedimentation of ignimbrites. Geol Soc Memoir 27:143 p

Cañón-Tapia E (2016) Reappraisal of the significance of volcanic fields. J Volcanol Geotherm Res 310:26–38

Cashman KV, Scheu B (2015) Magmatic fragmentation. In: Sigurdsson H, Houghton B, SR MN, Rymer H, Stix J (eds) Encyclopedia of Volcanoes, 2nd edn. Academic Press, Elsevier, USA, pp 459–472

Cashman KV, Sturtevant B, Papale P, Navon O (2000) Magmatic fragmentation. In: Houghton B, McNutt SR, Rymer H, Stix J (eds) Sigurdsson H. Academic Press, Encyclopedia of Volcanoes, pp 421–430

Cediel F, Shaw RP, Caceres C (2003) Tectonic assembly of the northern Andean block. In: Bartolini C, Buffer RT, Blickwede J (eds) The Circum-Gulf of Mexicoan the Caribbean: hydrocarbon habitats, basin information, and plate tectonics, vol 79. AAPG Memoir, pp 815–848

Cortés M, Angelier J, Colletta B (2005) Paleostress evolution of the northern Andes (Eastern Cordillera of Colombia): implications on plate kinematics of the South Caribbean region. Tectonics 24:27

De Silva S, Lindsay JM (2015) Primary volcanic landforms. In: Sigurdsson H, Houghton B, SR MN, Rymer H, Stix J (eds) Encyclopedia of volcanoes, 2nd edn. Academic Press, Elsevier, USA, pp 273–297

Feininger T (1970) The Palestina Fault, Colombia. Geol Soc Am Bull 81: 1201–1216

Gardner JE, Thomas RME, Jaupart C, Tait S (1996) Fragmentation of magma during plinian volcanic eruptions. Bull Volcanol 58:144–162

Gómez-Tapias J, Nivia Á, Montes NE, Almanza MF, Alcárcel FA, Madrid CA (2015) Notas explicativas: Mapa Geológico de Colombia. In: Gómez J, Almanza MF (Eds), Compilando la geología de Colombia: Una visión a 2015. Servicio Geológico Colombiano, Publicaciones Geológicas Especiales 33:9–33

González PD (2008) Texturas de los cuerpos ígneos. Asociación Geológica Argentina:172–196

González H (1990) Mapa geológico de Caldas, escala 1: 250.000. Memoria Explicativa. INGEOMINAS, Medellín, 62 p

Heiken G (1972) Morphology and petrography of volcanic ashes. Geol Soc Am Bull 83:1931–1988

Heiken G (1974) An atlas of volcanic ash. Smithson Contrib Earth Sci 12: 38–101

Houghton BF, Wilson CJN (1989) A vesicularity index for pyroclastic deposits. Bull Volcanol 51:451–462

Idárraga-García J, Kendall JM, Vargas CA (2016) Shear wave anisotropy in Northwest South America and its link to the Caribbean and Nazca subduction geodynamics. Geochem Geophys Geosyst 17:3655–3673

Irvine TNJ, Baragar WRA (1971) A guide to the chemical classification of the common volcanic rocks. Can J Earth Sci 8:523–548

Kereszturi G, Németh K (2012) Monogenetic basaltic volcanoes: genetic classification, growth, geomorphology and degradation. INTECH Open Access Publisher, 64 p

Kretz R (1983) Symbols for rock-forming minerals. Am Mineral 68:277–279

Le Bas MJ, Le Maitre RW, Streckeisen A, Zanettin B (1986) A chemical classification of volcanic rocks based on the total alkali-silica diagram. J Petrol 27:745–750

Le Maitre RW, Streckeisen A, Zanettin B, Le Bas MJ, Bonin B, Bateman P (eds) (2002) Igneous rocks: a classification and glossary of terms: recommendations of the International Union of Geological Sciences Subcommission on the Systematics of Igneous Rocks. Cambridge University Press, 254 p

Lonsdale P (2005) Creation of the Cocos and Nazca plates by fission of the Farallon plate. Tectonophysics 404:237–264

Martí J, López C, Bartolini S, Becerril L, Geyer A (2016) Stress controls of monogenetic volcanism: a review. Front Earth Sci 4:106

Martí J, Geyer A, Aguirre-Díaz G, Pedrazzi D, Bolós X (2017) Basaltic ignimbrites in monogenetic volcanism: the example of La Garrotxa volcanic field. Bull Volcanol 79:article 33. https://doi.org/10.1007/s00445-017-1113-0

Martí J, Groppelli G, Da Silveira AB (2018) Volcanic stratigraphy: a review. J Volcanol Geotherm Res 357:68–91

Maya M (2001) Distribución, facies y edad de las rocas metamórficas en Colombia. Instituto de Investigación e Información Geocientífica. Minero - Ambiental y Nuclear. Ministerio de Minas y Energía, Colombia, 57 p

Maya M, González H (1995) Unidades litodémicas en la Cordillera Central de Colombia, Instituto de Investigación e Información Geocientífica, Ministerio de Minas y Energía, Colombia, Boletín Geológico 35:43–57

McGee LE, Smith IEM (2016) Interpreting chemical compositions of small scale basaltic systems: a review. J Volcanol Geotherm Res 325:45–60

Monsalve ML (2015) Vulcanismo en el área geotérmica de San Diego (Caldas), informe de avance. Servicio Geológico Colombiano, informe interno:80 p

Monsalve ML, Arcila M (2016). Volcán El Escondido: ¿Evidencia de la prolongación norte del vulcanismo activo en Colombia? Abstract, Memorias Simposio 100 años del Servicio Geológico Colombiano

Monsalve ML, Rueda JB (2015) Vulcanismo como fuente de calor en el área geotérmica de San Diego (Caldas). XV Congreso Colombiano de Geología, 2015 "Innovar en Sinergia con el Medio Ambiente" Bucaramanga, Colombia agosto 31 – septiembre 5, 2015

Monsalve ML, Ortiz ID, Norini G (2019) El Escondido, a newly identified silicic quaternary volcano in the NE region of the northern volcanic segment (Central Cordillera of Colombia). J Volcanol Geotherm Res 383:47–62

Morrissey M, Zimanowski B, Wohletz K, Buettner R (2000) Phreatomagmatic fragmentation. In: Houghton B, McNutt SR, Rymer H, Stix J (eds) Sigurdsson H. Academic Press, Encyclopedia of Volcanoes, pp 431–446

Murcia HF, Borrero CA, Pardo N, Alvarado GE, Arnosio M, Scolamacchia T (2013) Depósitos volcaniclásticos: Términos y conceptos para una clasificación en español. Revista Geological de América Central 48:15–39

Murcia H, Borrero C, Németh K (2017) Monogenetic volcanism in the Cordillera Central of Colombia: unknown volcanic fields associated with the northernmost Andes' volcanic chain related subduction [Abstract]. EGU General Assembly 2017, April 23-28 Vienna, Austria

Murcia H, Borrero C, Németh K (2019) Overview and plumbing system implications of monogenetic volcanism in the northernmost Andes' volcanic province. J Volcanol Geotherm Res 383:77–87

Németh K (2010) Monogenetic volcanic fields: origin, sedimentary record, and relationship whit polygenetic volcanism. In: Cañón-Tapia E, Szakács A (Ed.), What is a volcano? Geological Society of America Special Paper 470:43–66

Peccerillo A, Taylor SR (1976) Geochemistry of Eocene calc-alkaline volcanic rocks from the Kastamonu area, northern Turkey. Contrib Mineral Petrol 58:63–81

Reimer PJ, Bard E, Bayliss A, Beck JW, Blackwell PG, Ramsey CB, Grootes PM (2013) IntCal13 and Marine13 radiocarbon age calibration curves 0–50,000 years cal BP. Radiocarbon 55:1869–1887

Rueda-Gutiérrez JB (2019) Aportes al conocimiento del Magmatismo de la Cordillera Central de Colombia en su Flanco Oriental: Área geotérmica de San Diego, Samaná, Caldas. Boletín de Geología 41:45–70

Sánchez-Torres L (2017) Caracterización de los productos volcánicos del volcán El Escondido y propuesta de un modelo evolutivo. Universidad de Caldas, Colombia, Bachelor thesis, 104 p

SGC (2017) Volcán El Escondido ¿Evidencia de la prolongación norte del vulcanismo activo en Colombia? (video file). Recovered from https://www.youtube.com/watch?v=_GP6eHNY7GI

Smith IEM, Németh K (2017) Source to surface model of monogenetic volcanism: a critical review. Geological Society, London, Special Publication 446:1–28

Suárez JE (2016) Mecanismos de transporte y acumulación durante las erupciones piroclásticas más explosivas, registradas al sur de Paipa, en la Cordillera Oriental de Colombia. Bachelor thesis, Universidad de Los Andes, Colombia, 130 p

Syracuse EM, Maceira M, Prieto GA, Zhang H, Ammon CJ (2016) Multiple plates subducting beneath Colombia, as illuminated by sesimicity and velocity from the joint inversion of seismic and gravity data. Earth Planet Sci Lett 44:139–149

Taboada A, Rivera LA, Fuenzalida A, Cisternas A, Philip H, Bijwaard H, Rivera C (2000) Geodynamics of the northern Andes: subductions and intracontinental deformation (Colombia). Tectonics 19:787–813

Toro AM, Delgado RA (2018) Volcán El Escondido (Samaná-Caldas, Colombia): Distibución de sus depósitos, características composicionales y texturales de los productos. Bachelor thesis, Universidad de Caldas, Colombia, 86 p

Valentine GA, Greeg TKP (2008) Continental basaltic volcanoes - processes and problems. J Volcanol Geotherm Res 177:857–873

Vallance JW, Iverson RM (2015) Lahars and their deposits. In: Sigurdsson H, Houghton B, SR MN, Rymer H, Stix J (eds) Encyclopedia of volcanoes, 2nd edn. Academic Press, Elsevier, USA, pp 649–664

Vargas CA, Mann P (2013) Tearing and breaking off of subducted slabs as the result of collision of the Panama Arc-Indenter with northwestern South America. Bull Seismol Soc Am 103:2025–2046

Villagómez D, Spikings R, Magna T, Kammer A, Winkler W, Beltrán A (2011) Geochronology, geochemistry and tectonic evolution of the Western and Central Cordilleras of Colombia. Lithos 125:875–896

Wagner LS, Jaramillo JS, Ramírez-Hoyos LF, Monsalve G, Cardona A, Becker TW (2017) Transient slab flattening beneath Colombia. Geophys Res Lett 44:6619–6623

White JDL, Valentine GA (2016) Magmatic versus phreatomagmatic fragmentation: absence of evidence is not evidence of absence. Geosphere 12:1478–1488

Zimanowski B, Büttner R, Dellino P, White JD, Wohletz KH (2015) Magma–water interaction and phreatomagmatic fragmentation. In: Sigurdsson H, Houghton B, SR MN, Rymer H, Stix J (eds) Encyclopedia of volcanoes, 2nd edn. Academic Press, Elsevier, USA, pp 473–484